



Green synthesis of Monteponite CdO nanoparticles by *Agathosma betulina* natural extract

F.T. Thema ^{a, b}, P. Beukes ^{a, b}, A. Gurib-Fakim ^{a, b}, M. Maaza ^{a, b, *}

^a UNESCO-UNISA Africa Chair in Nanosciences-Nanotechnology, College of Graduate Studies, University of South Africa, Muckleneuk Ridge, P.O. Box 392, Pretoria, South Africa

^b Nanosciences African Network (NANOAFNET), iThemba LABS-National Research Foundation, 1 Old Faure Road, Somerset West 7129, PO Box 722, Somerset West, Western Cape, South Africa



ARTICLE INFO

Article history:

Received 10 April 2015

Received in revised form

20 May 2015

Accepted 25 May 2015

Available online 20 June 2015

ABSTRACT

This contribution reports on the synthesis and the main physical properties of CdO nanoparticles synthesized for the first time by a completely green process using *Agathosma betulina* plant extract as an effective bio-oxidizing/bio-reducing agent. The surface/interface and volume room temperature properties by HRSEM, EDS, XRF, XRD, ATR-FTIR, Raman, XPS and Photoluminescence are reported.

© 2015 Elsevier B.V. All rights reserved.

Keywords:

Green synthesis

Transparent conducting oxides

Cadmium oxide

Nanoparticles

Agathosma betulina's extract

1. Introduction

Nano-scaled Cadmium oxide (CdO) have attracted special interest due to their unique optical transparency combined with a significant electronic conductivity, a property which was known as back as 1907 [1]. More precisely, CdO is a III–IV n-type semiconductor with a direct large and a narrow indirect band gaps ranging within 2.2–2.5 eV and 1.36–1.98 eV respectively [2,3]. The n-type conduction is attributed to its native oxygen vacancies and cadmium interstitials. Its average electron mobility is of the order $531 \text{ cm}^2 \text{ V}^{-1} \text{ s}^{-1}$ with a significant linear refractive index of about 2.49, conjugated to a high optical transparency in the visible spectral solar range [4–7]. Consequentially, it is considered as one of the most attractive Transparent Conducting Oxides (TCOs) as the ZnO family. It is an ideal candidate for several optoelectronics applications including solar cells, phototransistors, photodiodes, and transparent electrodes for gas sensors and flat panel displays based devices [8–15]. As-grown CdO n-type films exhibit a large electron

concentration higher than $10^{19}/\text{cm}^3$ [16]. This type of conductivity refers to rare cases where native defects, localized impurities and surface states can be donors in n-type or acceptors in p-type materials [17–19]. This is believed to be due to the location of defect level at ~1.15 eV above the conduction band (CB) in CdO. As a result, the Fermi energy at the free CdO surface is always pinned at this level [20]. This is similar to the situation observed in the well-known narrow bandgap InN based materials [21]. The high free electron concentration of CdO materials also results in a blue shift in the optical absorption edge due to the Burstein–Moss effect [22,23]. In recent years, many researchers have focused on CdO based nanomaterial due to their versatile applications in optoelectronics and TCOs sector. Reduction in the dimensionality of such materials from the 3-D bulk phases to the 0-D nanoparticles can lead to enhanced properties favored by quantum size effects and additional mesoscopic effects.

Yet, it is associated to a certain degree of toxicity in relation to cadmium content itself, extensive physical and chemical techniques have been used to prepare nanostructured CdO. In this regard, epitaxial CdO thin films, and highly crystalline micro-whiskers, nano-needles, nano-belts, nano-cubes, nano-clusters, nano-wires, nano-rods, and nanoparticles have been synthesized [24–36]. Hitherto, these physical/chemical methods are very

* Corresponding author. Nanosciences African Network (NANOAFNET), iThemba LABS-National Research Foundation, 1 Old Faure Road, Somerset West 7129, PO Box 722, Somerset West, Western Cape, South Africa

E-mail address: Maaza@tlabs.ac.za (M. Maaza).

effective; they are complex, and environmentally not friendly in view of the required energy balance and/or generated waste. To the best of our knowledge, green synthesis of nano-scaled CdO was never reported so far. However, it was demonstrated that such an attractive approach is successful in the synthesis of noble metallic nanoparticles, Au and Ag mainly as well as some limited oxides [37,38].

This contribution reports for the first time on the synthesis and the main physical properties of highly crystalline Monteponite CdO nanoparticles by a green chemistry process using *Agathosma betulina* natural extract as an effective oxidizing/reducing agent. The physical characteristics of such CdO nanoparticles engineered without any additional standard bases/acids, are investigated by high resolution scanning electron microscopy, energy dispersive X-Ray spectroscopy, X-rays fluorescence, X-rays diffraction, attenuated total reflection-Fourier transform infrared, Raman and X-rays photon spectroscopies in addition to room temperature photoluminescence to confirm their Monteponite CdO nature.

2. Synthesis: green process via *Agathosma betulina* natural extract

As it is mentioned above, the originality of this contribution resides in demonstrating for the first time the possibility to synthesize CdO nanoparticles by green chemistry process. More explicitly, natural extract from the *Agathosma betulina* was used to bio-oxidize/bio-reduce several cadmium based salts including CdNO₃, CdCl₂, CdSO₄, and Cd-Ammonium hydrate. This communication reports on the green reduction of Cd(NO₃)₂·4H₂O as a proof of the concept of synthesis of pure Monteponite CdO nanoparticles.

Agathosma betulina, as is scientifically labeled, is a plant commonly known as Buchu, Bucco, iBuchu, Boegoe, or round leave of Buch in vernacular names [39]. This plant is a sprouting shrub to 1.5 m height with about 20 mm long leaves in average, with broad but less than twice as long as wide (widest in the upper half). Rounded apex which curves backwards [40]. The flowers have five white or pale purple petals, solitary and star shaped. This plant is restricted to the Cederberg Mountains of the Western Cape Province of South Africa and Tulbagh in the South to Citrusdal and Clanwilliam in the North [40,41]. *Agasthma betulina* chemical composition is shown in Table 1 as reported below.

Dry leaves of *Agathosma betulina* were supplied from the Western Cape Province-South Africa. The identity of *Agasthma betulina* plant was confirmed by the taxonomy experts in the herbarium of the Department of Life Sciences at the University of Western Cape. The 15 g of *Agathosma betulina* leaves were weighed and washed with distilled water at room temperature. The leaves were then immersed in the de-ionized water to extract the green dye and heated at about ~100 °C for an hour. The dye extract solution was filtered twice to eliminate residual solids if there were any. The hydrated cadmium nitrate Cd(NO₃)₂·4H₂O was considered

Table 1
Major bioactive compounds in the *Agathosma betulina* natural extract.

Flavonoids:	Pelargonidin-3,5-diglucoside(I), Cyanidin-3,5-diglucoside(II), Kaempferol(III);
Monoterpeneoids:	β-pinene(IV) 1,8-cineol; Pyrogallol(V)
Tannins:	Catechol(VI); Betulinic acid(VII), α-amyrin(VIII)
Triterpenoids:	Oleanolic acid(IX) β-sitosterol(X)

as cadmium precursor. This Cd(NO₃)₂·4H₂O was of analytical grade reagent and was used without any further purification in view of its relatively high solubility. In a typical procedure, the required amount of cadmium nitrate (6.0 g) was homogeneously mixed with 100 ml of *Agathosma betulina* solution. This mixture was then heated at temperature of 100 °C for two hours while tightly closed. The cadmium nitrate dissolved and resulted into a fine precipitate. The as prepared deposit was washed with deionized water repeatedly, centrifuged using a Lasec Sigma 2–6 unit at 1000 rps for 10 min. The mixture was dried in an oven at 100 °C and then annealed in an open furnace at 500 °C for 2 h.

3. Results & discussion

3.1. Morphology & microscopy observations

Fig. 1 reports a typical High Resolution Scanning Electron Microscopy (HRSEM) of the annealed CdO nanoparticles at 500 °C for 2 h. The powdered sample consists of agglomerated clusters of various sizes up to 100 nm in spatial extension. More accurate analysis, yet within the limits of resolution of the HRSEM unit, one could still notice that the clusters are formed by smaller aggregated quasi-spherical nanoparticles with diameters as small as 8 nm.

3.2. Elemental analysis

Fig. 2 reports a typical Energy Dispersive X-Ray Spectroscopy (EDS) spectrum collected with an Oxford instruments X-Max solid state silicon drift detector operating at 20 keV of the annealed CdO nanoparticles at 500 °C for 2 h. In addition to the expected Cd (3.15 and 3.45 eV) and O (0.52 eV) peaks, one can distinguish several additional peaks related to Au, Pd, Si, and Carbon. Excluding the Carbon (0.27 eV), these later ones correspond to the Au–Pd surface coating used to minimize the charge effects on the surface of the pelletized sample and the Si substrate respectively. The presence of carbon can be assigned to residue formed during the Cd nitrate green reaction with the *Agasthma betulina* natural extract. To confirm the CdO nature of the nanoparticles, X-Ray Fluorescence

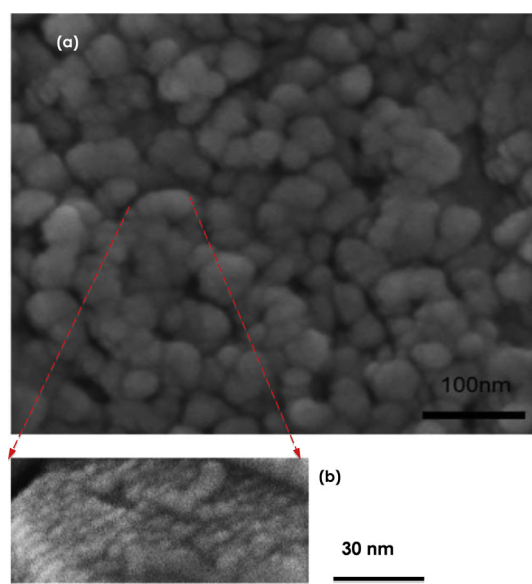


Fig. 1. (a) Typical High resolution Scanning Electron Microscopy of the annealed CdO nanoparticles at 500 °C for 2 h. (b) Zoom on a single nanoparticle showing the internal morphology consisting of several nano-grains.

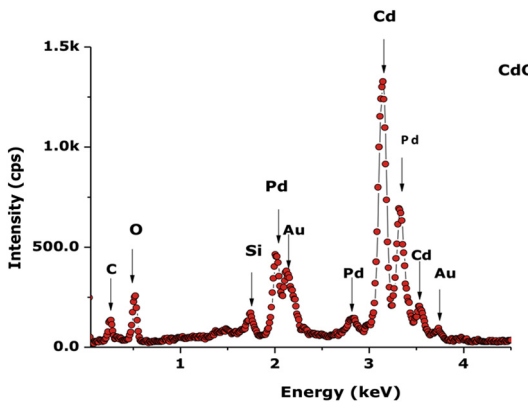


Fig. 2. Typical Energy Dispersive X-Ray Spectroscopy (EDS) spectrum of the annealed CdO nanoparticles at 500 °C for 2 h.

(XRF) investigations were carried out at various spots of the pellet. Fig. 3 shows a typical energy-dispersion XRF spectrum of the annealed CdO nanoparticles at 500 °C for 2 h. The spectrum exhibits the double Cd L-band located within 3.133–3.528 keV without any additional element [42], this reaffirms the pure chemical form of the CdO nanoparticles.

3.3. Structural & crystallographic analysis

The standard conditions stable phase of CdO is a cubic phase within the space group Fm 3m and a unit-cell parameter $a = 4.694 \text{ \AA}$. Fig. 4 reports a typical XRD profile of the CdO synthesized particles. Such a powder X-ray diffractometry was carried out using computer controlled X'pert PRO PANalytical diffractometer with a monochromatic CuK α 1 radiation (wavelength 1.5406 Å), operating at a voltage of 40 KV and a current of 35 mA, in the angular range 2Θ of 20–75 deg. Five Bragg peaks are observed (Table 2) only highlighting on the high degree of symmetry of the investigated crystallites so far. More accurately, the diffraction peaks can be indexed as a cubic CdO structure (JCPD card no 05–0640) with an average lattice parameter $\langle a \rangle = 4.701 \text{ \AA}$. No peak from pure Cd or other Cd–O phases can be found in the XRD spectrum. This sustains the single phase of the prepared product i.e. pure CdO. The 3 peaks positioned before the (111) CdO intense Bragg diffraction are assigned to Carbon which could have originated from the synthesis process itself as highlighted in the

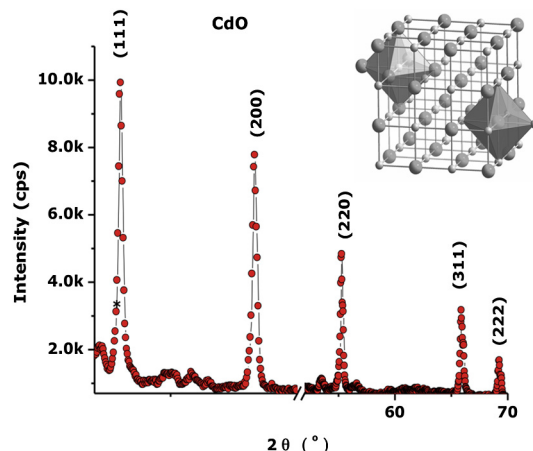


Fig. 4. Room temperature X-Rays Diffraction profile of the CdO synthesized nanoparticles at 500 °C for 2 h (CuK α 1 radiation = 1.5406 Å).

previous section. The Debye-Scherrer approximation $\langle \phi_{\text{Particles}} \rangle - 0.9 \lambda / \Delta \Theta_{1/2} \cos \theta_B$ allows to estimate the average diameter of the CdO nanocrystals ($\phi_{\text{Particles}}$) which was found to be ranging from 25 to ~50 nm in a good agreement with the previous HRSEM observations. Likewise, Table 2 shows that the ratio $(d_{\text{hkl}}^{\text{Exp}} - d_{\text{hkl}}^{\text{Bulk}}) / d_{\text{hkl}}^{\text{Bulk}}$ is less than 0.03% for all hkl reticular plans except for the (111) direction. For this orientation specifically, the ratio is about ~+7.5% indicating that (111) reticular plans are under elongation conditions.

3.4. Vibrational properties

To validate once more the Monteponite nature of the synthesized CdO particles and their purity, Attenuated Total Reflection-Fourier Transform Infrared spectroscopy (ATR-FTIR) studies were performed at room temperature. Fig. 5 reports the typical ATR-FTIR spectrum of the pressed powder in the spectral range of 400–4000 cm $^{-1}$. The IR transmission is plotted versus the wavenumber so to single out the major absorptions observed at lower wavenumbers. As one can observe, we distinguish mainly 2 relatively intense absorptions centered at approximately 3435 and 1623 cm $^{-1}$. They are associated to standard OH stretching and H₂O bending modes respectively. These OH/H₂O functional groups content could be related to surface adsorbed water or atmospheric water vapor. The ATR-FTIR spectrum shows no residual organic compounds such as NO₃⁻ after filtration and centrifugation. The less intense peaks located at 462, 542, 780, and 1107 cm $^{-1}$ are all associated to the stretching Cd–O modes [43–47]. The presence of these four characteristic Cd–O stretching modes supports the phase purity of the Monteponite CdO nature of the nanoparticles.

From Raman view point, bulk CdO is the only II_b-VI compound with a cubic structure of the NaCl type. This crystal structure has O_h space group symmetry [48,49]. The corresponding CdO major transverse and longitudinal optical modes are located within the Raman spectral range of 291–1000 cm $^{-1}$ [50,51]. Fig. 6 reports the room temperature Raman spectrum using the 532 nm excitation laser line with an average excitation power of 2.48 mW in the spectral range of 200–1000 cm $^{-1}$. One can distinguish 3 major peaks centered at ~259.3, ~390.4 and ~937.5 cm $^{-1}$. An additional peak at about ~329.9 cm $^{-1}$ located as a shoulder of the most intense ~390.4 cm $^{-1}$ peak. Based on the experimental and theoretical results of Bilz et al., Popovic et al., Ashrati et al. as well as Cusco et al., the 4 modes are assigned to the transverse and longitudinal modes of cubic CdO with a possible internal compressive stress which might be surface effect induced.

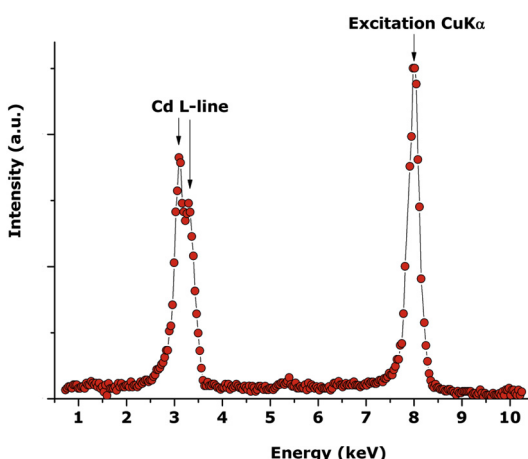


Fig. 3. Typical X-Ray Fluorescence spectrum of the annealed CdO nanoparticles at 500 °C for 2 h using CuK α radiation as an excitation source.

Table 2

Major XRD characteristics of the various Bragg diffraction peaks.

Miller indexation (<i>hkl</i>)	θ_{bulk} (rad)	d_{bulk} (Å)	d_{exp} (Å)	$d_{exp}-d_{bulk}/d_{bulk}$	$\Delta\Theta_{1/2}$ FWHM (10^{-2} rad)	$\langle \phi_{Particles} \rangle$ (nm)	a(nm)
(111)	0.288	2.7118	2.762	0.7561	0.378	38.2	4.676
(200)	0.334	2.3488	2.348	-0.0003	0.394	37.3	4.696
(220)	0.482	1.6603	1.660	-0.0001	0.501	31.3	4.695
(311)	0.575	1.4159	1.412	-0.0031	0.604	27.4	4.682
(222)	0.605	1.3549	1.355	-0.0000	0.635	26.6	4.693

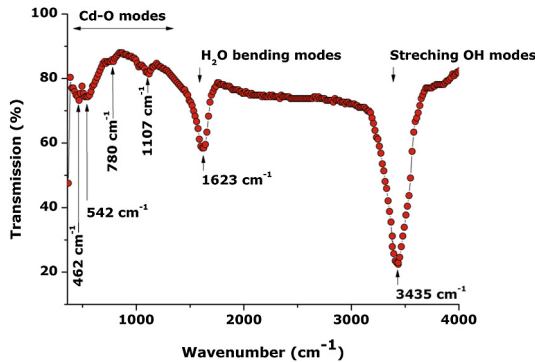


Fig. 5. Typical ATR-FTIR spectrum of the pressed powder consisting of CdO synthesized nanoparticles at 500 °C for 2 h in the spectral range of 400–4000 cm^{-1} .

3.5. Surface properties

As a preliminary conclusion, and from the combined HRSEM, EDS, XRF, XRD, ATR-FTIR and Raman results, one could conclude on the phase purity of the synthesized CdO nanoparticles. To gain information on their surface chemistry, X-rays Photoemission Spectroscopy (XPS) investigations were therefore, carried out. Indeed, the species covering the surface of the nanoparticles can be detected by the kinetic-energy analysis of both valence-band and inner-shell photoelectrons. To obtain information on the surface properties of the CdO nanoparticles, the binding energies of Cd (3d) and O (1s) electrons were measured by analyzing the XPS spectra. These investigations were acquired using a constant 50 eV pass energy mode, in 0.1 eV increments at 50 ms dwell time with the signal averaged for at hundreds of regular scans. The XPS system was equipped with a dual Mg K α –Al K α anode for photo excitation.

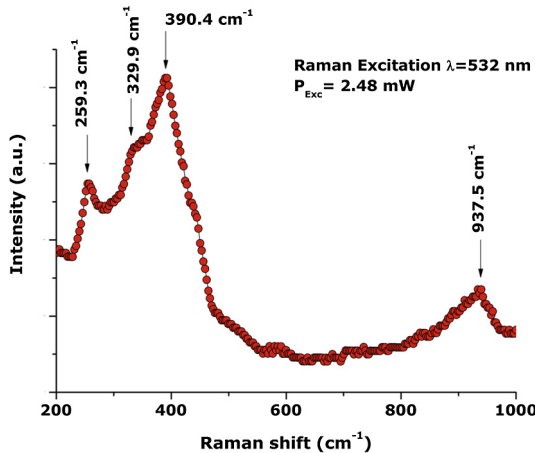


Fig. 6. Typical room temperature Raman spectrum using the 532 nm excitation laser line with an average excitation power of 2.48 mW in the spectral range of 200–1000 cm^{-1} .

Fig. 7 reports a typical core level spectra of the Cd (3d) that consists of the Cd 3d_{5/2} and Cd 3d_{3/2} spin orbit components that are located at binding energy of 405.0 and 411.7 eV, respectively which are in agreement with those reported by Gulino et al., and Gujar et al. [52,53]. Such a binding energy of the Cd (3d) is attributed to the Cd²⁺ bonding state and hence the CdO single phase of the synthesized samples.

As a follow up of the EDS, XRF, XRD, ATR-FTIR, Raman and XPS investigations, room temperature photoluminescence (PL) studies were conducted to estimate the nature and the density of the defects and ion deficiencies if any. Indeed the photoluminescence phenomenon is directly related to electronic structure and transitions. Differences in the electronic behavior between bulk semiconductor and their nano-scaled counterpart arise due to the difference in the electronic density of states. An excitation wavelength $\lambda_{exc} = 325$ nm from a He–Cd laser source was used to conduct the room temperature PL measurements. Fig. 8 reports the PL spectrum of the annealed CdO nanoparticles at 500 °C for 2 h. One can distinguish a broad VIS emission centered at about ~501 nm with a shoulder at ~585 nm in addition to a relatively sharp UV emission at ~409 nm and 2 additional less intense peaks at about ~376 nm and ~395 nm respectively. The UV emission peak at 409 nm is well known to be related to the exciton emission. The mechanism of VIS emission centered at 501 nm within the spectral

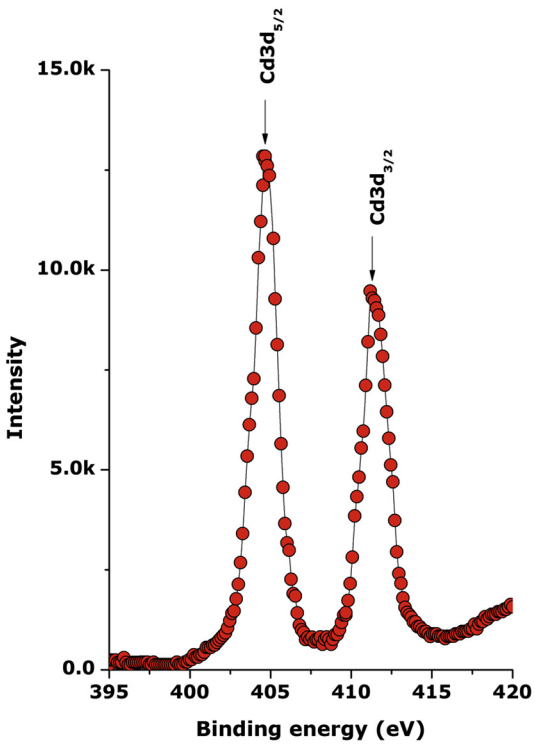


Fig. 7. Typical core level spectra of the Cd (3d) that consists of the Cd 3d_{5/2} and Cd 3d_{3/2} spin orbit components.

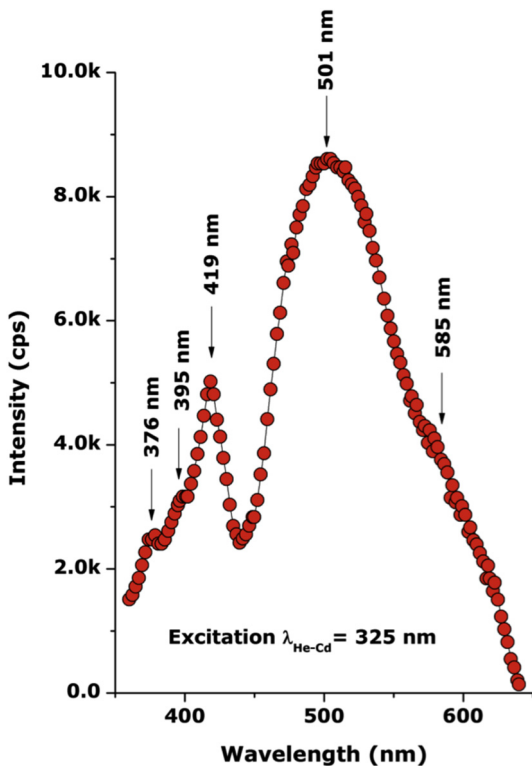


Fig. 8. Room temperature photoluminescence spectrum of the annealed CdO nanoparticles at 500 °C for 2 h. The excitation wavelength $\lambda_{\text{exc}} = 325 \text{ nm}$ from a He–Cd laser source was used.

range of 450–600 nm, is suggested as mainly due to the presence of various point defects, either extrinsic or intrinsic, which can easily form recombination centres [54–57]. The emissions centered at $\sim 376 \text{ nm}$ and $\sim 395 \text{ nm}$ are attributed to deep level emissions usually appearing due to surface effects [58–66].

4. Conclusions

The synthesis of single phase highly crystalline CdO nanoparticles by green novel and environmental friendly pathway using the natural extract of *Agathosma betulina*'s extract as an effective oxidizing/reducing chemical agent was demonstrated. A thermal annealing of $\sim 500 \text{ }^{\circ}\text{C}$ during $\sim 2 \text{ h}$ under normal air conditions allows to obtain highly crystallized single phase CdO nanoparticles as substantiated by the HRSEM, EDS, XRF, XRD, ATR-FTIR, Raman, XPS, and PL investigations. The follow up study will consist of identifying the physical/chemical mechanisms and the dynamic formation of the CdO nanoparticles during the interaction of the Cadmium salt precursor and the *Agathosma betulina*'s natural extract compounds. More specifically, the bioactive compound(s) would be identified. In addition, the synthesis of less stable oxides such as CdO₂ nanoparticles is being investigated.

Acknowledgments

This research program was generously supported by grants from the National Research Foundation of South Africa (NRF) (NRF 2014 MM 4200220), the UNESCO-UNISA Africa Chair in Nanosciences & Nanotechnology (U2ACN2 2014-52259064), iThemba LABS (iTl 2014 MM), the Organization of Women in Science for the Developing World (OWSDW) (OWSDW 2014 4200220) and the Abdus Salam ICTP via the Nanosciences African Network (NANOAFNET) (ICTP AFNET 2014 63), The Academy of Sciences for the Developing

World (TWAS) (TWAS 2014 MM 42002200) as well as the African Laser Centre (ALC) (ALC 2014 MM) to whom we are grateful.

References

- [1] K. Kaviyarasu, E. Manikandan, P. Paulraj, S.B. Mohamed, J. Kennedy, *J. Alloys Compd.* 593 (2014) 67–70.
- [2] A. Tadjarodi, M. Imani, H. Kerdari, *Mater. Res. Bull.* 48 (2013) 935–942.
- [3] H. Kohler, *Solid State. Comms* 11 (1972) 1687.
- [4] J. Polleuse, N. Pinna, M. Antonietti, M. Niedorberger, *Adv. Mater.* 16 (2004) 436.
- [5] N. Pinna, U. Wild, J. Urban, *Adv. Mater.* 15 (2003) 329.
- [6] K. Kaviyarasu, D. Sajan, M. Selvakumar, *J. Phys. Chem. Solids* 73 (2012) 1396–1400.
- [7] N. Pinna, M. Willinger, K. Weiss, J. Urban, *IR. Schlog, Nano. Lett.* 3 (2003) 1131.
- [8] L.M. Su, N. Grote, F. Schmitt, *Jpn. Electron Lett.* 20 (1984) 716.
- [9] R. Kondo, H. Okimura, Y. Sakai, *J. Appl. Phys.* 10 (1971) 1547.
- [10] F.A. Benko, F.P. Koffyberg, *Solid State Commun.* 57 (1986) 901.
- [11] D.R. Lide, *CRC Handbook of Chemistry & Physics*, seventyseventh ed., CRC Press, 1996, pp. 12–97.
- [12] C. Sravani, K.T.R. Reddy, O.M. Hussain, P.J. Reddy, *J. Sol. Energy. Soc. India* 1 (1996) 6.
- [13] L.M. Su, N. Grote, F. Schmitt, *Electron. Lett.* 20 (1984) 716.
- [14] R. Kondo, H. Okimura, Y. Sakai, *Jpn. J. Appl. Phys.* 10 (1971) 1547.
- [15] F.A. Benko, F.P. Koffyberg, *Solid State Commun.* 57 (1986) 901.
- [16] Q. Zhou, Z. Ji, B. Hu, C. Chen, L. Zhao, C. Wang, *Mater. Lett.* 61 (2007) 531.
- [17] C. McGuinness, C.B. Stagarescu, P.J. Ryan, J.E. Downes, D. Fu, K. Smith, R.G. Eggleton, *Phys. Rev. B* 68 (2003) 165104.
- [18] C.G. Van de Walle, *Phys. Rev. Lett.* 85 (2000) 1012.
- [19] A. Peles, A. Janotti, C.G.V. de Walle, *Phys. Rev. B* 78 (2008) 035204.
- [20] L. Colakerol, L.F. Piper, P.D.C. King, A. Schleife, J. Zuniga-Perez, Per-Anders Glans, T. Learmonth, A. Federov, T.D. Veal, F. Fuchs, V. Munoz-Sanjose, F. Bechstedt, C.F. McConville, K.E. Smith, *Phys. Rev. B* 78 (2008) 165127.
- [21] W. Walukiewicz, J.W. Ager III, K.M. Yu, Z. Lilienthal-Weber, J. Wu, S.X. Li, R.E. Jones, J.D. Enderling, *J. Phys. D* 39 (2006) R85.
- [22] M. Altwein, H. Finkenrath, C. Konak, J. Stuke, G. Zimmerer, *Phys. Status Solidi* 29 (1968) 203.
- [23] E. Burstein, *Phys. Rev.* 93 (1954) 632.
- [24] X. Liu, C. Li, S. Han, J. Han, C. Zhou, *Appl. Phys. Lett.* 82 (2003) 1950.
- [25] B.S. Zou, V.V. Volkov, Z.L. Wang, *Chem. Mater.* 11 (1999) 3037.
- [26] X. Wu, R. Wang, B. Zou, L. Wang, S. Liu, J. Xu, *J. Mater. Res.* 13 (1998) 604.
- [27] M.D. Uplane, P.N. Kshirsagar, B.J. Lokhande, C.H. Bhosale, *Mater. Chem.* 64 (2000) 75.
- [28] M. Yan, M. Lane, C.R. Kannewurf, R.P.H. Chang, *Appl. Phys. Lett.* 78 (2001) 2342.
- [29] A. Gulino, P. Dapporto, P. Rossi, I. Fragala, *Chem. Mater.* 14 (2002) 1441.
- [30] A. Gulino, G. Tabbi, *Appl. Surf. Sci.* 245 (2005) 322.
- [31] N. Kopanarova, Z. Zlatev, D. Genchev, G.J. Popovich, *Mater. Sci.* 29 (1994) 103.
- [32] X. Liu, C. Li, S. Han, J. Han, C. Zhou, *Appl. Phys. Lett.* 82 (2003) 1950.
- [33] Z.W. Pan, Z.R. Dai, Z.L. Wang, *Science* 291 (2001) 1947.
- [34] J.H. Kim, Y.C. Hong, H.S. Uhm, *J. Appl. Phys.* 46 (2007) 4351.
- [35] B.S. Zou, W. Volkov, Z.L. Wang, *Chem. Mater.* 11 (1999) 3037.
- [36] M. Ghosh, C.N.R. Rao, *Chem. Phys. Lett.* 393 (2004) 493.
- [37] J.K. Sharma, M.S. Akhtar, G. Sing, *J. Alloys Compd.* 632 (2015) 321–325.
- [38] B. Mohapatra, S. Kuriakose, S. Mohapatra, *J. Alloys Compd.* 637 (2015) 119–126.
- [39] C.A. Smith, *Mem. Botanical Surv. S. Afr.* 35 (1966) 576.
- [40] T. Brendler, D. Philips, A. Gurib-Fakim, J.N. Elöff, *African Herbal Pharmacopoeia*, AAMPS Publishing, Mauritius, 2010, ISBN 9789990389098, p. 289.
- [41] B.E. van Wyk, B. van Oudtshoorn, N. Gericke, *Medicinal Plants of South Africa*, Briza Publication, Pretoria, South Africa, 2013, pp. 63–66.
- [42] A.A. Dakhel, *Thin Solid Films* 518 (2010) 1712–1715.
- [43] I. K. Gurumurugan, D. Mangalaraj, S.K. Narayandass, *J. Electron. Mater.* 25 (1996) 765.
- [44] T. Kuo, M.H. Huang, *J. Phys. Chem. B* 110 (2006) 13717–13721.
- [45] M. Benhaliliba, C.E. Benouis, A.S. Tiburcio, *J. Lumin* 132 (2012) 2653–2658.
- [46] M.A. Flores, P.R. Castaneda, D.G. Torres, S.A. Toms, A.J.G. Mendoza, A.O. Zelaya, *J. Lumin* 130 (2010) 2500–2504.
- [47] Z.V. Popovic, G. Stanisic, R. Kostic, *Phys. Stat. Sol.(b)* 165 (1991) K109.
- [48] H. Bilz, D. Strauch, R.K. Wehner, *Handbook. Phys.*, in: *Licht und Materie* Id, vol. XXVIIId, Springer-Verlag, Berlin, 1984, p. 157.
- [49] A.S. Aldwayyan, F.M. Al-Jekhudad, M. Al-Noaimi, T.B. Hadda, M. Suleiman, I. Warand, *Int. J. Electrochem. Sci.* 8 (2013) 10506–10514.
- [50] A. Ashrafi, K. Ostrikov, *Appl. Phys. Lett.* 98 (33119) (2011) 1–3.
- [51] R. Cusco, J. Ibanez, N. Domenech-Amador, L. Artus, J. Zuniga-Perez, V. Munoz-Sanjose, *J. Appl. Phys.* 107 (063519) (2010) 1–4.
- [52] A. Gulino, F. Castelli, P. Dapporto, P. Rossi, I. Fragala, *Chem. Mater.* 14 (2002) 704.
- [53] T.P. Gujar, V.R. Shinde, Woo-Young Kim, Kwang-Deog Jung, C.D. Lokhande, Oh-Shim Joo, *Appl. Surf. Sci.* 254 (2008) 3813–3818.
- [54] T. Aswani, V. Pushpa Manjari, B. Babu, Sk Muntaz Begum, G. Rama Sundari, K. Ravindranadh, R.V.S.S.N. Ravikumar, *J. Mol. Struct.* 1063 (2014) 178–183.
- [55] M. Benhaliliba, C.E. Benouis, A. Tiburcio-Silver, F. Yakuphanoglu, A. Avila-Garcia, A. Tavira, R.R. Trujillo, Z. Mouffak, *J. Lumin* 132 (2012) 2653.

- [56] B.J. Jin, H.S. Woo, S. Im, S.H. Bae, S.Y. Lee, *Appl. Surf. Sci.* 521 (2001) 169.
- [57] N. Niehl, *J. Lumin.* 24 (1981) 335.
- [58] D.J. Seo, *J. Korean Phys. Soc.* 45 (2004) 1575.
- [59] A. Hosseiniyan, A.R. Mahjoub, M. Movahedi, *J. Appl. Chem. Res.* 4 (2010) 14.
- [60] N. Clament Sagaya Selvam, R. Thinesh Kumar, K. Yogeenth, L. John Kennedy, Sekaran, J. Judith Vijaya, *Powder Technol.* 211 (2011) 250.
- [61] P.K. Sharma, M. Kumar, A.C. Pandey, *J. Nanopart. Res.* 13 (2011) 1629.
- [62] S. Muthukumaran, R. Gopalakrishnan, *Opt. Mater.* 34 (2012) 1946.
- [63] T.M. Kim, S.L. Cooper, M.V. Klein, B.T. Jonker, *Phys. Rev. B* 49 (1994) 1732.
- [64] D.E. Billing, R.J. Dudley, B.J. Hathaway, A.A.G. Tomlinson, *J. Chem. Soc. A* 6 (1971) 91.
- [65] K. Kaviyarasu, E. Manikandan, J. Kennedy, M. Jayachandran, *J. Mater. Lett.* 120 (2014) 243–245.
- [66] J. Li, Y. Chem, Y.C. Zhang, J.G. Duan, *Adv. Mater. Res.* 1035 (2014) 321–324.